Mussel Adhesive Hot Paper

DOI: 10.1002/ange.201406099

In Vivo Residue-Specific Dopa-Incorporated Engineered Mussel Bioglue with Enhanced Adhesion and Water Resistance**

*Byeongseon Yang, Niraikulam Ayyadurai, Hyungdon Yun, Yoo Seong Choi, Byeong Hee Hwang, Jun Huang, Qingye Lu, Hongbo Zeng, and Hyung Joon Cha**

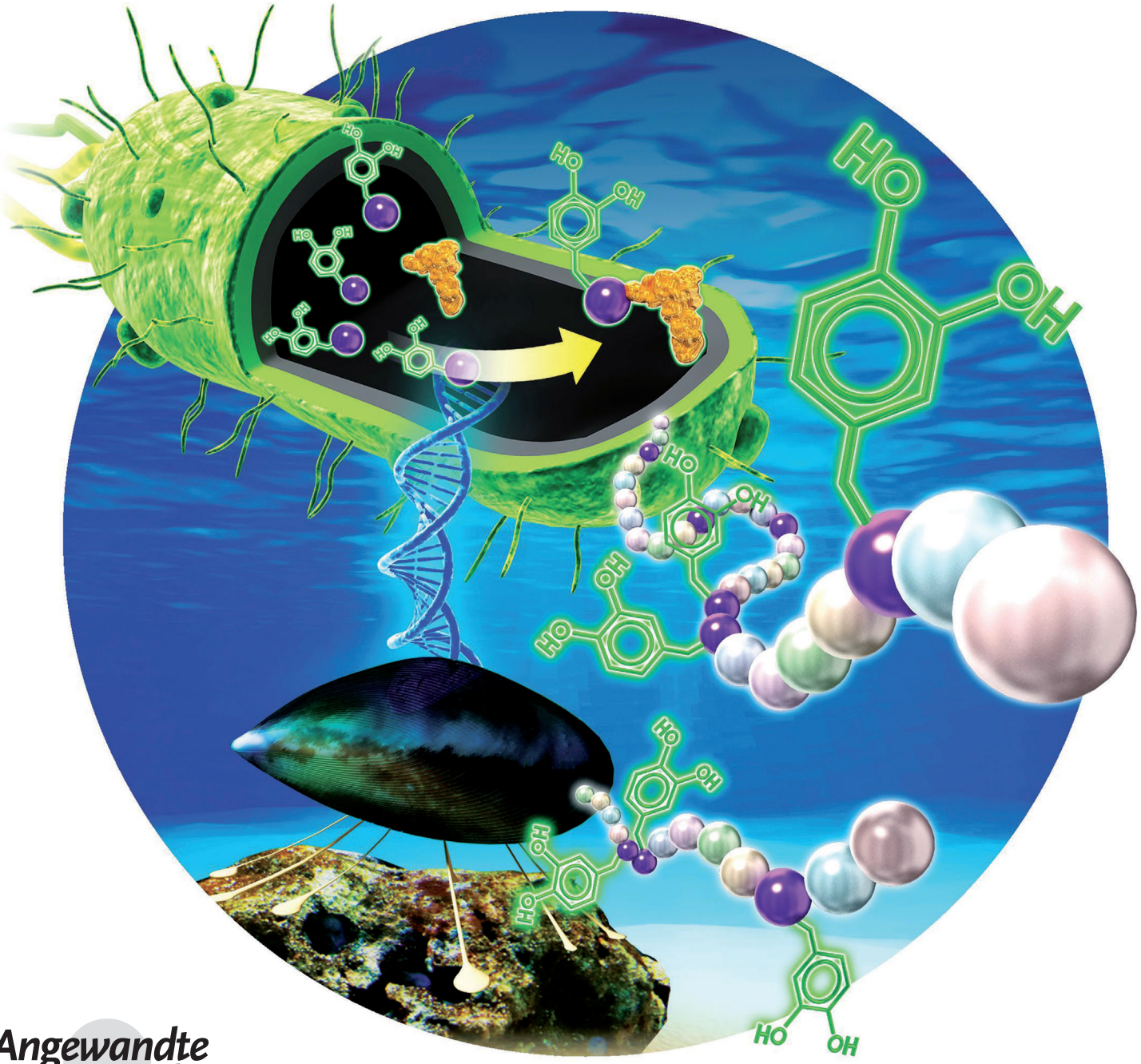

Abstract: *Misaminoacylation of 3,4-dihydroxyphenylalanine (Dopa) molecules to $tRNA^{Tyr}$ by endogenous tyrosyl-tRNA synthetase allowed the quantitative replacement of tyrosine residues with a yield of over 90 % by an in vivo residue-specific incorporation strategy, to create, for the first time, engineered mussel adhesive proteins (MAPs) in Escherichia coli with a very high Dopa content, close to that of natural MAPs. The Dopa-incorporated MAPs exhibited a superior surface adhesion and water resistance ability by assistance of Dopa-mediated interactions including the oxidative Dopa cross-linking, and furthermore, showed underwater adhesive properties comparable to those of natural MAPs. These results propose promising use of Dopa-incorporated engineered MAPs as bioglues or adhesive hydrogels for practical underwater applications.*

3,4-Dihydroxyphenylalanine (Dopa), which is a hydroxylated form of tyrosine residue, has been suggested to be the key factor for rapid and strong underwater adhesion due to its mediation of various interactions such as bidentate hydrogen bonding, complexes with metals and metal oxides, cation–π and/or π–π interaction, and oxidative cross-linking as it is oxidized to Dopa-quinone.[1] Mussel adhesive protein (MAP) is one example of how Dopa chemistry is used as the core underwater adhesion principle.[2] In particular, MAP type 3 (fp-3) and type 5 (fp-5), surface adhesion components adjacent to the adhesion interface, have extremely high Dopa content of 10–20 and ca. 25 mol %, respectively.[2a,3] The biosynthesis of recombinant MAPs in *Escherichia coli* system was a good approach to overcome the availability limitation that results from the extremely low yield of natural MAPs extraction from mussel feet.[4] However, Dopa incorporation always follows as the biggest problem because lack of Dopa in recombinant MAPs critically limits the underwater adhesion. To transform tyrosine residues into Dopa molecules, an in vitro mushroom tyrosinase treatment has commonly been conducted.[4b,5] However, this process exhibits a low (< 15 %) modification yield.[4b] Several other methods have been attempted,[6] but there are no epochal strategies to significantly enhance the Dopa content of recombinant MAPs to levels similar to those in natural MAPs.

A method that can incorporate noncanonical amino acids into proteins is being developed in the field of biotechnology.[7] In particular, the residue-specific method allows the incorporation of a noncanonical amino acid instead of a specific canonical amino acid.[7b,8] Previously, the residue-specific Dopa incorporation was investigated in an *E. coli* cell-free system[9] and in *E. coli* cells to create a new function such as conjugate chemistry[10] or metal-binding chemistry in biosensor applications.[11] However, this residue-specific Dopa incorporation method has not been tried in biomimetic protein biosynthesis. Natural MAPs originally contain as much as 25 mol % Dopa, which is responsible for the characteristic properties of strong adhesion and water resistance. Thus, we expected that the residue-specific noncanonical amino acid incorporation will be an appropriate method to engineer the Dopa chemistry observed in the natural MAPs into the recombinant MAPs to mimic and retain the advantages of Dopa.

A schematic illustration of the expression of the in vivo residue-specific Dopa-incorporated engineered recombinant MAP is shown in Figure 1 a. The affinity of tyrosyl-tRNA synthetase (TyrRS) for Dopa was reported to be competitive

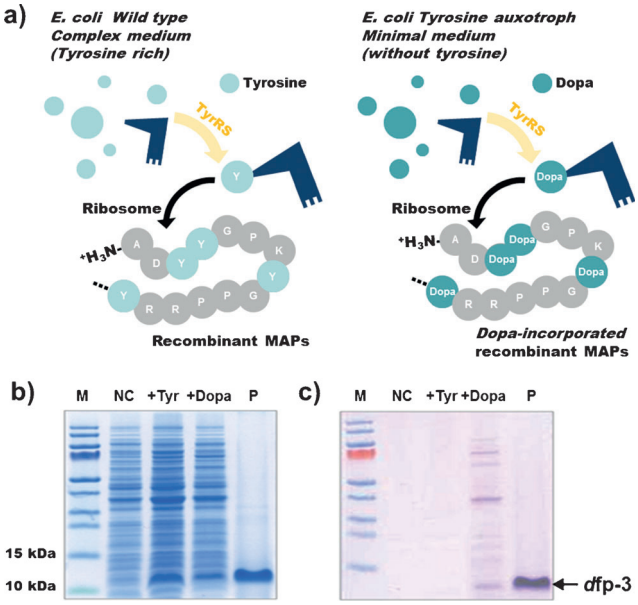

Figure 1. a) Schematic illustration of the in vivo residue-specific incorporation of Dopa into recombinant MAP. Analyses of the expression and purification of *d*fp-3 in *E. coli* using 15 % Tricine-SDS-PAGE with b) Coomassie staining and c) NBT staining. Lanes: M, protein molecular weight marker; NC, expressed with only 19 amino acids as a negative control; + Tyr, expressed with 19 amino acids and tyrosine; + Dopa, expressed with 19 amino acids and Dopa; P, purified protein.

[*] B. Yang, Dr. B. H. Hwang, Prof. H. J. Cha
Department of Chemical Engineering
Pohang University of Science and Technology
Pohang 790-784 (Korea)
E-mail: hjcha@postech.ac.kr
Dr. N. Ayyadurai
Department of Biotechnology, Central Leather Research Institute
Chennai 600-020 (India)
Prof. H. Yun
Department of Bioscience and Biotechnology, Konkuk University
Seoul 143-701 (Korea)
Prof. Y. S. Choi
Department of Chemical Engineering
Chungnam National University
Daejon 305-764 (Korea)
J. Huang, Dr. Q. Lu, Prof. H. Zeng
Department of Chemical and Materials Engineering
University of Alberta
Edmonton, Alberta, T6G 2V4 (Canada)

[**] Financial support was provided by the Marine Biotechnology program funded by the Ministry of Oceans and Fisheries, Korea. B.Y. acknowledges the support from the Global Ph.D. Fellowship funded by the National Research Foundation of Korea. H.Z. acknowledges the support from the Natural Sciences and Engineering Research Council of Canada and J.H. acknowledges the support from Alberta Innovates Graduate Student Scholarship.

Supporting information for this article is available on the WWW under http://dx.doi.org/10.1002/anie.201406099.

with that for tyrosine, showing an approximately two order of magnitude difference.[12] Thus, the supplemented Dopa will be charged to the $tRNA^{Tyr}$ by the endogenous TyrRS after the *E. coli* tyrosine auxotroph cells reach a stationary phase in minimal medium as the small amount of tyrosine that was initially added is depleted. Finally, Dopa will be co-translationally introduced into the recombinant MAPs in the *E. coli*. The tricine sodium dodecyl sulfate–polyacrylamide gel electrophoresis (SDS-PAGE) analysis clearly showed successful expression of in vivo residue-specific Dopa-incorporated recombinant fp-3 (*d*fp-3) (+Dopa) (Figure 1b). Approximately 3–5 mg L^{-1} of purified *d*fp-3 was obtained from a 400 mL-scale culture after Ni-NTA affinity chromatographic purification. A similar yield (3–5 mg L^{-1}) was also obtained for purified in vivo residue-specific Dopa-incorporated recombinant fp-5 (*d*fp-5) (see Figure S1a in the Supporting Information).

With the redox-cycling nitroblue tetrazolium (NBT) staining which detects proteins containing Dopa and Dopaquinone,[13] *d*fp-3 was clearly stained in a blue-purple band (Figure 1c). From qualitative comparison of NBT-stained dot blots, *d*fp-3 showed intense color development that was much stronger than that of tyrosinase-modified recombinant fp-3 (*m*fp-3), demonstrating that the residue-specific Dopa incorporation method greatly increased the Dopa content in the recombinant fp-3 (Figure S2a). In the case of *d*fp-5, the same pattern was also observed (Figure S1b and S3a).

Amino acid composition analysis determined the specific Dopa incorporation yield of *d*fp-3 (Table 1 and Figure S2b). Of the total 10 tyrosine residues, 94% were occupied by Dopa, resulting in a Dopa content of 16.5 mol%; the Dopa content of *d*fp-3 was significantly higher than that of *m*fp-3, which had a modification yield of 14% and a Dopa content of 2.6 mol%. Through matrix-assisted laser desorption ionization-time of flight mass spectrometry (MALDI-TOF MS) analysis, we additionally confirmed clear mass difference closely corresponding to the Dopa incorporation yields calculated from amino acid analysis (Table 1 and Figure S2c). Naturally extracted fp-3 has almost 100% replacement of tyrosine residues with Dopa molecules, for a Dopa content of ca. 20 mol%. Thus, we found that the Dopa content of *d*fp-3 was similar to that of naturally extracted fp-3. The specific Dopa incorporation yield of *d*fp-5 was also determined to be 94% with a Dopa content of 22.9 mol% (Figure S3b and Table S1), which was greatly improved compared with that of *m*fp-5. Additionally, the N-terminal amino acid sequence of *d*fp-3 was analyzed to be H_2N-Ala-Asp-Dopa-Dopa-Gly-Pro-Lys-Dopa-Gly, which were identical to the expected nine N-terminal amino acids of natural fp-3, thus confirming that Dopa successfully and only substituted for tyrosine.

Table 1: Dopa incorporation yield, Dopa content, and molecular weight of recombinant fp-3 MAPs.

MAP	Dopa incorporation yield [%]	Dopa content [mol%]	MALDI mass[a] (Dopa numbers)
fp-3	0.0	0.0	6652.9 (0)
*m*fp-3	14.2	2.6	6652.4 (0) 6668.6 (1) 6684.8 (2)
*d*fp-3	94.0	16.5	6796.2 (9) 6812.4 (10)

[a] Intense mass signals in the MALDI-TOF MS spectrum. Numbers in parentheses indicate corresponding numbers of sites occupied by Dopa.

To evaluate the effects of Dopa incorporation on the properties of the engineered MAPs, three analyses were performed: direct surface-coating analysis for the surface adhesion ability in dry conditions, quartz crystal microbalance (QCM) analysis for the water resistance, and surface forces apparatus (SFA) analysis for the underwater surface adhesion ability. For a comparative evaluation, fp-3, *m*fp-3, and *d*fp-3 were used. First, through direct surface-coating analysis, we surmise that the Dopa content of the protein plainly enhances the surface adhesion ability (Figure 2). Although there was no

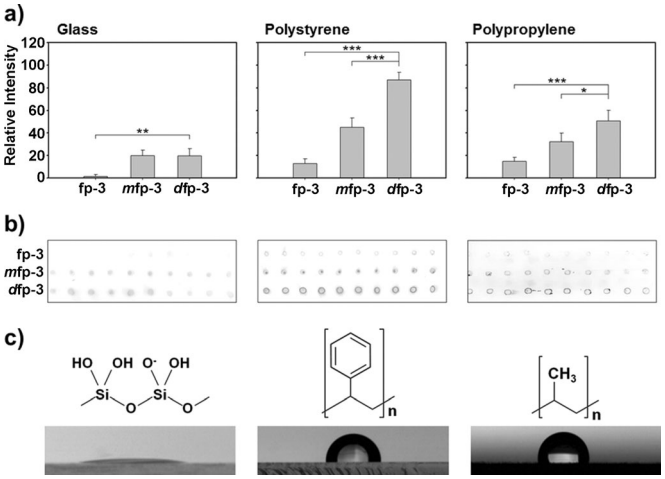

Figure 2. Direct surface-coating analysis for the surface adhesion ability of *d*fp-3 in the dry condition. a) Analyzed intensities and b) images of stained dots. Each measurement of the dot intensity was repeated for at least 10 dots and averaged. The values and error bars represent the means and standard deviation, respectively; statistical significance is designated by the symbols $*p < 1\times10^{-3}$, $**p < 1\times10^{-6}$, and $***p < 1\times10^{-9}$. c) Contact angle measurement.

big difference between *m*fp-3 and *d*fp-3 on the glass surface, a significant increase in the surface adhesion ability along with Dopa content was clearly observed on polystyrene and polypropylene surfaces (Figure 2a,b). Regardless of hydrophilicity of the three surfaces determined by contact angle measurement: glass (18°) > polystyrene (83°) > polypropylene (97°) (Figure 2c), the largest increase in surface adhesion ability was found on the polystyrene surface, which might be related to cation–π and/or π–π interaction because *d*fp-3 contains many positively charged amino acids and Dopa which has a benzene ring.

Next, the water resistance of *d*fp-3 was compared with that of fp-3 and *m*fp-3 through QCM analysis. To provide water resistance, 25 mM sodium periodate was used to induce oxidative cross-linking of the Dopa after surface adhesion on a gold surface. To observe the water resistance, the protein-spotted gold-coated crystal was washed with 0.1M acetic acid

for 1 h, and then, the resonant frequency change was measured. As expected, *d*fp-3 was best able to remain on the surface (Figure 3a). The resonant frequency change of *d*fp-3 after washing was 1709 ± 199 Hz; this value was 24.8-fold higher than that of fp-3 (69 ± 1 Hz, $p < 0.001$) and even

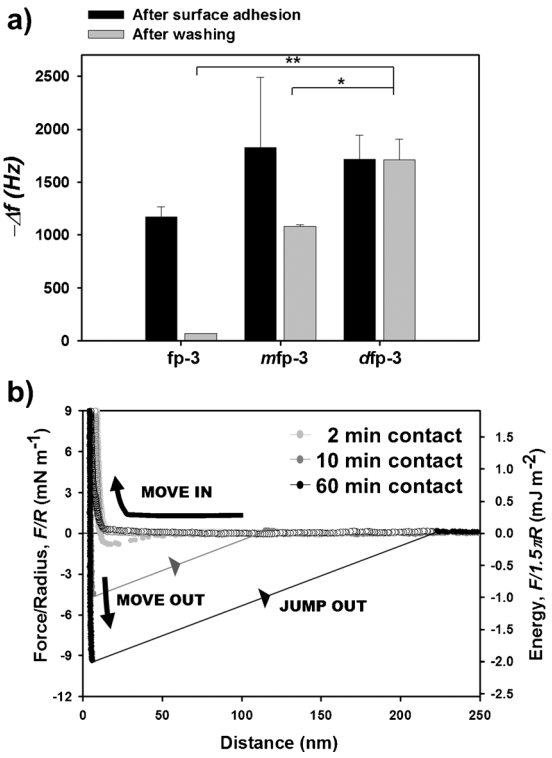

Figure 3. a) QCM analysis for the water resistance of *d*fp-3. Each measurement was repeated at least twice and averaged for a given sample. The values and error bars represent the means and standard deviation, respectively; statistical significance is designated by the symbols $*p < 0.05$ and $**p < 0.001$. b) SFA analysis for the underwater surface adhesion ability of *d*fp-3 against a bare mica surface in 0.1 M acetic acid with 0.25 M KNO_3 at pH 3. The normalized forces, F/R, are shown on the left ordinate, whereas the corresponding interaction energies per unit area (defined by $F/1.5\pi R$) are on the right ordinate.

1.6-fold higher than that of *m*fp-3 (1079 ± 17 Hz, $p < 0.05$). Moreover, the resonant frequency change before and after washing was analyzed to investigate how much protein remained on the surface relative to the amount of initially adhered proteins. The *d*fp-3 retained 99.5% with almost no protein loss during washing, showing its excellent water resistance. On the other hand, all Dopa-deficient fp-3 proteins were mostly washed out, and subsequently retained only 5.9%. *m*fp-3 remained 59% even after Dopa cross-linking. For water resistance, both the surface and cohesive adhesions are important.[1f] The Dopa oxidation induced by periodate makes MAPs exhibit strong cohesive interactions via intramolecular and intermolecular Dopa cross-linkings between MAPs;[2b,4b] effective cross-linking in the bulk of MAPs will not be dispersed or solubilized in water environment.

SFA measures force between surfaces; through SFA analysis, the surface adhesion force of naturally extracted MAPs have been studied in underwater environments in the manner reported previously.[3,14] Mica surface is commonly used as a target surface because it is atomically smooth, chemically inert, and biologically relevant.[14a,d] The underwater adhesive property of *d*fp-3 to mica surface was investigated by SFA analysis as a normal force against the mica–mica separation distance in 0.1 M acetic acid with 0.25 M KNO_3 at pH 3, where Dopa auto-oxidation is effectively prevented. As a result, *d*fp-3 showed strong underwater adhesion with adhesion energy of 2.0 mJ m^{-2} with 60 min contact time (Figure 3b). This result is comparable to the previous SFA analysis of natural fp-3 (Table 2).[14e] Also, *d*fp-5 showed strong underwater adhesion (3.7 mJ m^{-2} with 60 min contact time) to the bare mica surface, which is also relatively comparable to the adhesion energy of natural fp-5[3] (Figure S4 and Table S2). Thus, we concluded that the adhesion abilities of the in vivo residue-specific Dopa-incorporated engineered MAPs in aqueous conditions were comparable to those of naturally extracted MAPs.

Table 2: Underwater surface adhesion of natural and engineered fp-3 MAPs measured using SFA analysis.[a]

Protein	Force/radius [mN m^{-1}]	Adhesion energy [mJ m^{-2}]	Ref.
natural fp-3	≈ -12	≈ 2.5[b]	[14e]
*d*fp-3	-9.4	2.0	this work

[a] Experimental condition: 0.1 M acetic acid with 0.25 M KNO_3, pH 3 with 60 min contact time. [b] Recalculated value according to $F_{ad} = 1.5\pi R W_{ad}$ for deformable surface.

Here, successful in vivo residue-specific Dopa incorporation was performed to create engineered MAPs containing a large amount of Dopa. The Dopa incorporation yield was over 90%, a large improvement over that of the commonly used conventional in vitro tyrosinase modification method with <15% yield. The reported method provided a more convenient production of Dopa-incorporated recombinant MAPs without any additional modification processes after the protein purification. More importantly, this was the first time that the recombinant MAPs were created with a high Dopa content (16.5 mol% for *d*fp-3 and 23 mol% for *d*fp-5) similar to that (20 mol% for fp-3 and 25 mol% for fp-5) of the natural MAPs. Using several analyses, we confirmed that the engineered MAPs with large amounts of Dopa showed greatly enhanced surface adhesion in dry and underwater environments and strong water resistance. Engineered MAPs have His_6-tag for facile affinity purification (Table S3). This additional histidine cluster might affect adhesive properties such as surface dependent adhesive interaction, metal ion dependent cohesive interaction, and cross-linking density.[2a,b,3] While other mussel-inspired chemical synthetic approaches such as dopamine and polyethylene glycol (PEG)-Dopa systems have focused only on Dopa chemistry,[15] the Dopa-incorporated biosynthetic MAP systems are on the basis of natural MAP sequence and can maintain the advantages from other amino acid residues involved in underwater mussel adhesion along with good biocompatibility and biodegradability. This work can further expand to

incorporate other modified residues, such as 4-hydroxyarginine for fp-3 and O-phosphoserine for fp-5,[16] for deeper insights on mussel adhesion mechanism study. Overall, the in vivo residue-specific Dopa-incorporated engineered MAPs with excellent underwater adhesion ability have great potential for use as adhesive/cohesive combined systems in various underwater applications such as bioglues and adhesive hydrogels with self-healing property derived from reversible Dopa-Fe^{3+} complexation (Figure S5).[17]

Received: June 10, 2014
Published online: September 1, 2014

Keywords: biomimetic synthesis · Dopa · mussel adhesive proteins · noncanonical amino acids · underwater bioadhesive

[1] a) T. H. Anderson, J. Yu, A. Estrada, M. U. Hammer, J. H. Waite, J. N. Israelachvili, *Adv. Funct. Mater.* **2010**, *20*, 4196 – 4205; b) H. Lee, N. F. Scherer, P. B. Messersmith, *Proc. Natl. Acad. Sci. USA* **2006**, *103*, 12999 – 13003; c) M. J. Sever, J. T. Weisser, J. Monahan, S. Srinivasan, J. J. Wilker, *Angew. Chem. Int. Ed.* **2004**, *43*, 448 – 450; *Angew. Chem.* **2004**, *116*, 454 – 456; d) Q. Lu, D. S. Hwang, Y. Liu, H. Zeng, *Biomaterials* **2012**, *33*, 1903 – 1911; e) H. Zeng, D. S. Hwang, J. N. Israelachvili, J. H. Waite, *Proc. Natl. Acad. Sci. USA* **2010**, *107*, 12850 – 12853; f) S. C. Nicklisch, J. H. Waite, *Biofouling* **2012**, *28*, 865 – 877.

[2] a) H. G. Silverman, F. F. Roberto, *Mar. Biotechnol.* **2007**, *9*, 661 – 681; b) H. J. Cha, D. S. Hwang, S. Lim, *Biotechnol. J.* **2008**, *3*, 631 – 638; c) T. J. Deming, *Curr. Opin. Chem. Biol.* **1999**, *3*, 100 – 105; d) J. H. Waite, *Integr. Comp. Biol.* **2002**, *42*, 1172 – 1180.

[3] B. P. Lee, P. B. Messersmith, J. N. Israelachvili, J. H. Waite, *Annu. Rev. Mater. Res.* **2011**, *41*, 99 – 132.

[4] a) Y. S. Choi, D. G. Kang, S. Lim, Y. J. Yang, C. S. Kim, H. J. Cha, *Biofouling* **2011**, *27*, 729 – 737; b) B. Yang, D. G. Kang, J. H. Seo, Y. S. Choi, H. J. Cha, *Biofouling* **2013**, *29*, 483 – 490.

[5] K. Marumo, J. H. Waite, *Biochim. Biophys. Acta.* **1986**, *872*, 98 – 103.

[6] a) S. Lim, K. R. Kim, Y. S. Choi, D.-K. Kim, D. Hwang, H. J. Cha, *Biotechnol. Prog.* **2011**, *27*, 1390 – 1396; b) Y. S. Choi, Y. J. Yang, B. Yang, H. J. Cha, *Microb. Cell Fact.* **2012**, *11*, 139.

[7] a) L. Wang, J. Xie, P. G. Schultz, *Annu. Rev. Biophys. Biomol. Struct.* **2006**, *35*, 225 – 249; b) J. A. Johnson, Y. Y. Lu, J. A. Van Deventer, D. A. Tirrell, *Curr. Opin. Chem. Biol.* **2010**, *14*, 774 – 780.

[8] A. J. Link, D. A. Tirrell, *Methods* **2005**, *36*, 291 – 298.

[9] K. Ozawa, M. J. Headlam, D. Mouradov, S. J. Watt, J. L. Beck, K. J. Rodgers, R. T. Dean, T. Huber, G. Otting, N. E. Dixon, *FEBS J.* **2005**, *272*, 3162 – 3171.

[10] N. Ayyadurai, N. S. Prabhu, K. Deepankumar, Y. J. Jang, N. Chitrapriya, E. Song, N. Lee, S. K. Kim, B. G. Kim, N. Soundrarajan, S. Lee, H. J. Cha, N. Budisa, H. Yun, *Bioconjugate Chem.* **2011**, *22*, 551 – 555.

[11] N. Ayyadurai, N. Saravanan Prabhu, K. Deepankumar, S. G. Lee, H. H. Jeong, C. S. Lee, H. Yun, *Angew. Chem. Int. Ed.* **2011**, *50*, 6534 – 6537; *Angew. Chem.* **2011**, *123*, 6664 – 6667.

[12] a) R. Calendar, P. Berg, *Biochemistry* **1966**, *5*, 1690 – 1695; b) G. Hogenauer, G. Kreil, H. Bernheimer, *FEBS Lett.* **1978**, *88*, 101 – 104.

[13] M. A. Paz, R. Fluckiger, A. Boak, H. M. Kagan, P. M. Gallop, *J. Biol. Chem.* **1991**, *266*, 689 – 692.

[14] a) J. Israelachvili, Y. Min, M. Akbulut, A. Alig, G. Carver, W. Greene, K. Kristiansen, E. Meyer, N. Pesika, K. Rosenberg, *Rep. Prog. Phys.* **2010**, *73*, 036601; b) Q. Lu, E. Danner, J. H. Waite, J. N. Israelachvili, H. Zeng, D. S. Hwang, *J. R. Soc. Interface* **2013**, *10*, 20120759; c) E. W. Danner, Y. Kan, M. U. Hammer, J. N. Israelachvili, J. H. Waite, *Biochemistry* **2012**, *51*, 6511 – 6518; d) Q. Lin, D. Gourdon, C. Sun, N. Holten-Andersen, T. H. Anderson, J. H. Waite, J. N. Israelachvili, *Proc. Natl. Acad. Sci. USA* **2007**, *104*, 3782 – 3786; e) J. Yu, W. Wei, E. Danner, J. N. Israelachvili, J. H. Waite, *Adv. Mater.* **2011**, *23*, 2362 – 2366.

[15] a) H. Lee, S. M. Dellatore, W. M. Miller, P. B. Messersmith, *Science* **2007**, *318*, 426 – 430; b) K. Huang, B. P. Lee, D. R. Ingram, P. B. Messersmith, *Biomacromolecules* **2002**, *3*, 397 – 406; c) C. E. Brubaker, H. Kissler, L. J. Wang, D. B. Kaufman, P. B. Messersmith, *Biomaterials* **2010**, *31*, 420 – 427.

[16] a) V. V. Papov, T. V. Diamond, K. Biemann, J. H. Waite, *J. Biol. Chem.* **1995**, *270*, 20183 – 20192; b) J. H. Waite, X. Qin, *Biochemistry* **2001**, *40*, 2887 – 2893.

[17] a) N. Holten-Andersen, M. J. Harrington, H. Birkedal, B. P. Lee, P. B. Messersmith, K. Y. Lee, J. H. Waite, *Proc. Natl. Acad. Sci. USA* **2011**, *108*, 2651 – 2655; b) B. J. Kim, D. X. Oh, S. Kim, J. H. Seo, D. S. Hwang, A. Masic, D. K. Han, H. J. Cha, *Biomacromolecules* **2014**, *15*, 1579 – 1585.